

Inhibition of mild steel corrosion in groundwater by pyrrole and thienylcarbonyl benzotriazoles

D. Gopi · K. M. Govindaraju ·
V. Collins Arun Prakash · V. Manivannan ·
L. Kavitha

Received: 7 January 2008 / Accepted: 12 September 2008 / Published online: 26 September 2008
© Springer Science+Business Media B.V. 2008

Abstract The inhibition efficiency of Zn^{2+} , 3-phosphonopropionic acid (3-PPA), benzotriazole (BTA) and two synthesized benzotriazole derivatives namely 1-(2-pyrrole carbonyl) benzotriazole (PCBT) and 1-(2-thienylcarbonyl) benzotriazole (TCBT) were evaluated as inhibitors for the corrosion of mild steel in ground water. The inhibition efficiencies of PCBT and TCBT in combination with Zn^{2+} and 3-PPA were also investigated and the results were compared with BTA. In order to study the corrosion rate and inhibition efficiency we employed potentiodynamic polarization and electrochemical impedance spectroscopy (EIS). Further characterization using Fourier transform infrared spectroscopy (FT-IR) and X-ray diffraction (XRD) demonstrates the adsorption of inhibitor and the formation of corrosion products on the mild steel surface, respectively. Combination of PCBT along with Zn^{2+} and 3-PPA shows better corrosion inhibition efficiency than other inhibitor combinations and the individual inhibitors.

Keywords Corrosion · Mild steel · Inhibition · Potentiodynamic polarization · Impedance · Benzotriazole

1 Introduction

It is well known that triazole-type compounds are good corrosion inhibitors for many metals and alloys in aggressive media [1–5]. For example, benzotriazole is an efficient inhibitor for iron [6] and copper [7–11]. Many phosphonic acid derivatives and phosphonates have been used as inhibitors for stainless steel and iron [12, 13]. In this paper, we report the corrosion behavior of mild steel in ground water medium in the presence and absence of synthesized benzotriazole derivatives namely PCBT and TCBT. Electrochemical techniques such as potentiodynamic polarization, electrochemical impedance and surface characterization techniques like FT-IR and XRD were performed to study the corrosion behavior. Furthermore, weight loss measurements were also performed to estimate the corrosion rate and inhibition efficiency and the results of the benzotriazole derivatives were compared with benzotriazole. Earlier investigation showed that, the addition of Zn^{2+} enhances the inhibition efficiency by synergism [14–16] and hence the synergistic effect of the benzotriazole derivatives (PCBT and TCBT) with Zn^{2+} and 3-PPA is also reported in this paper.

2 Experimental

2.1 Synthesis of benzotriazole derivatives

Both the benzotriazole derivatives (PCBT and TCBT) were synthesized by adopting literature procedures [17–19] and the products were characterized by FT-IR and NMR. The structures of the compounds are given in Fig. 1.

D. Gopi (✉) · K. M. Govindaraju · V. Collins Arun Prakash ·
V. Manivannan
Department of Chemistry, Periyar University, Salem 636 011,
Tamilnadu, India
e-mail: periyaruniversitygopi@yahoo.co.in

L. Kavitha
Department of Physics, Periyar University, Salem 636 011,
Tamilnadu, India

Name	Abbreviation	Structure
Benzotriazole	BTA	
1-(2-Thienylcarbonyl)-benzotriazole	TCBT	
1-(2-Pyrrolicarbonyl)-benzotriazole	PCBT	
3-Phosphonopropionic acid	3-PPA	

Fig. 1 Structures and names of the benzotriazole derivatives and phosphonic acid derivative

2.2 Specimen preparation

Mild steel samples with the composition C-0.13%, P-0.032%, Si-0.014%, S-0.025%, Mn-0.48% and balance Fe were used. For each electrochemical study, specimens of size 1.0 cm × 1.0 cm × 0.3 cm were cut, embedded in epoxy resin and mechanically polished with silicon carbide papers (from grades 120 to 1,200) followed by then washing with double distilled water, degreasing with acetone and drying at room temperature.

For weight loss measurements metal specimens of 4.0 cm × 2.0 cm × 0.2 cm dimension were used. Samples of ground water were collected at 10 different locations and were tested for corrosiveness by the Langlier saturation index (LSI) [20]. A sample that was corrosive in nature was chosen as the test solution for all the experiments; the typical analysis of this electrolyte is given in Table 1.

2.3 Weight loss measurements

Mild steel specimens in triplicate were immersed in ground water at room temperature for each inhibitor concentration

Table 1 Analysis of ground water

Parameter	Value
pH	6.78
Temperature	28 °C
Total hardness	332 ppm
Alkalinity	316 ppm
TDS	586 ppm
LSI	−0.02
RSI	6.82

LSI, Langelier Saturation Index

RSI, Ryznar Stability Index

for 7 days. The specimens were removed, rinsed in double distilled water and acetone then kept in a desiccator. Then the weight loss was determined in order to calculate the inhibition efficiency using the formula,

$$IE(\%) = \frac{W_0 - W_i}{W_0} \times 100 \quad (1)$$

where, W_0 and W_i are the weight loss in the absence and presence of inhibitor respectively.

2.4 Electrochemical studies

All electrochemical measurements were performed using an Electrochemical Workstation (Model No: CHI 760, CH Instruments, USA) and all experiments were carried out at a constant temperature of 28 ± 2 °C with ground water as electrolyte. A platinum electrode and a saturated calomel electrode (SCE) were used as auxiliary and reference electrodes, respectively and the working electrodes comprised the mild steel specimens of 1 cm² area. The tip of the reference electrode was positioned very close to the surface of working electrode by the use of a fine Luggin capillary in order to minimize ohmic potential drop. The remaining uncompensated resistance was reduced by using the electrochemical workstation.

2.4.1 Potentiodynamic polarization measurements

The potentiodynamic polarization studies were carried out at a scan rate of 0.01 mV s^{−1}. In all cases the OCP was established first and then the polarization measurements were carried out. The polarization curves for mild steel specimens in the test solution with and without various concentrations of inhibitor were recorded from −1,200 to 0 mV.

2.4.2 Electrochemical impedance (EIS) studies

Electrochemical impedance studies were carried out with the same setup used for potentiodynamic polarization studies. The applied AC perturbation signal was about 10 mV within the frequency range 100 kHz to 1 Hz.

2.5 Surface examinations

The mild steel specimens were immersed in inhibitor solution for 7 days after which they were taken out and dried. Surface investigation of the metal and the adsorbed inhibitor on the specimens were carried out by FT-IR and XRD. The FT-IR spectra of the films were recorded using a Perkin-Elmer FT-IR spectrophotometer and a Nexus-670 while the corrosion products were identified by X-ray diffraction (model: XRD-Bruker D8 Advance-Germany).

3 Results and discussion

3.1 Weight loss measurements

All the inhibitors were tested for seven different concentrations to estimate the weight loss and inhibition efficiency as presented in Table 2. There is a significant decrease in the corrosion rate with increase in concentration of each inhibitor and the extent of inhibition depends on the nature and concentration of the inhibitor. The optimum concentration was evaluated based on inhibition efficiency; for BTA, TCBT and PCBT, these are 18, 16 and 12 ppm respectively. BTA, TCBT and PCBT have a maximum inhibition efficiency of 65.0, 70.7 and 74.4% respectively. Other individual inhibitors such as Zn²⁺ and 3-PPA showed a maximum inhibition efficiency of 67.7 and 65.9% respectively while the combination of PCBT + Zn²⁺ + 3-PPA had a maximum inhibition efficiency of 90.1%.

3.2 Electrochemical measurements

3.2.1 Potentiodynamic polarization measurements

Potentiodynamic polarization studies of mild steel in ground water in the absence and presence of inhibitors were carried out. For 3-PPA, TCBT and PCBT studies were made at different concentrations from 6 to 24 ppm, while for Zn²⁺ the concentrations were varied from 30 to 120 ppm (Table 3). The inhibition efficiency increases appreciably with increase in inhibitor concentration up to the optimum level, after which it decreases. The optimum concentrations were evaluated based on the inhibition

efficiency and the combination of benzotriazole derivatives with Zn²⁺ and 3-PPA was also studied.

The polarization curves obtained in the absence and presence of various inhibitors are shown in Figs. 2 and 3. Comparison of the curves shows that, with respect to the blank, increasing the concentration of the additive PCBT up to the optimum level gave a consistent decrease in both anodic and cathodic current densities. PCBT acts as a mixed-type inhibitor with predominant anodic effect. The addition of zinc along with PCBT does not modify the mechanism of the process but slightly alters the shape of the anodic curve due to the predominant cathodic inhibition of zinc. The presence of active sites such as aromatic rings and heteroatoms in the benzotriazole derivatives are responsible for the adsorption. Their corrosion inhibition efficiencies are directly proportional to the amount of adsorbed inhibitor.

The potentiodynamic polarization parameters of mild steel immersed in ground water for all the inhibitor systems are given in Tables 3 and 4. From the corresponding polarization curves presented in Fig. 2, the corrosion potential shows a clear tendency to be more negative for all the individual inhibitors except 3-PPA for which the shift in the E_{corr} value is positive. All the individual inhibitors except 3-PPA and PCBT act as mixed type inhibitors with moderate control of the cathodic reaction. In the presence of benzotriazole and its derivatives, the cathodic and anodic curves shift towards lower current density (i_{corr}) with a slight negative shift in the potential, indicating that BTA, TCBT and PCBT are all of mixed type. The corrosion potential in the presence of benzotriazole derivatives and Zn²⁺ shows a shift in the negative direction when compared with its absence. This

Table 2 Corrosion rate of mild steel in ground water in the presence and absence of optimum concentration of the various inhibitors—weight loss measurement

S. No.	Inhibitor	Inhibitor concentration (ppm)	Corrosion rate (mpy)	Inhibition efficiency (%)
1	Blank	–	6.6	–
2	BTA	18	2.3	65.0
3	TCBT	16	1.9	70.7
4	PCBT	12	1.7	74.4
5	Zn ²⁺	75	2.1	67.7
6	3-PPA	12	2.2	65.9
7	BTA + Zn ²⁺	18 + 75	1.7	73.8
8	TCBT + Zn ²⁺	16 + 75	1.5	77.9
9	PCBT + Zn ²⁺	12 + 75	1.3	80.1
10	PCBT + 3-PPA	12 + 12	1.2	81.8
11	TCBT + Zn ²⁺ + 3-PPA	16 + 75 + 12	1.0	84.5
12	PCBT + Zn ²⁺ + 3-PPA	12 + 75 + 12	0.6	90.1

Table 3 Potentiodynamic polarization parameters of mild steel in ground water containing various concentrations of BTA, TCBT, PCBT, Zn²⁺ and 3-PPA

S. No.	Inhibitor	Inhibitor concentration/ ppm	E_{corr} (mV)	i_{corr} ($\mu\text{A cm}^{-2}$)	Corrosion rate (mpy)	Inhibition efficiency (%)
1	Blank	–	–640	12.59	6.0	–
2	BTA	12	–662	6.30	3.0	50.0
		14	–650	5.25	2.5	58.3
		16	–673	4.78	2.3	62.0
		18	–680	4.36	2.1	65.4
		20	–676	4.47	2.1	64.5
		22	–690	5.01	2.4	60.2
		24	–672	5.62	2.7	55.4
3	TCBT	10	–795	7.41	3.5	41.1
		12	–744	6.12	2.9	51.4
		14	–740	4.38	2.1	65.2
		16	–775	3.55	1.7	71.8
		18	–760	4.74	2.2	62.4
		20	–725	5.60	2.6	55.5
		22	–745	6.49	3.1	48.5
4	PCBT	6	–715	7.08	3.3	43.8
		8	–785	6.30	3.0	50.0
		10	–715	5.82	2.7	53.8
		12	–720	3.09	1.5	75.5
		14	–748	4.16	2.0	66.9
		16	–770	5.71	2.7	54.6
		18	–774	6.96	3.3	44.7
5	Zn ²⁺	30	–655	6.02	2.8	52.2
		45	–690	5.62	2.7	55.4
		60	–750	4.26	2.0	66.2
		75	–705	3.98	1.9	68.4
		90	–740	4.16	2.0	66.9
		105	–740	4.78	2.3	62.0
		120	–690	5.25	2.5	58.3
6	3-PPA	6	–635	7.71	3.6	38.8
		8	–652	7.50	3.5	40.4
		10	–651	5.52	2.6	56.2
		12	–620	4.26	2.0	66.2
		14	–610	5.31	2.5	57.9
		16	–655	6.36	3.0	49.5
		18	–680	7.12	3.4	43.4

shift demonstrates the cathodic inhibiting effect of the combination of both the benzotriazole derivatives with Zn²⁺. With the aid of Tafel extrapolation the corrosion inhibition efficiencies of BTA, TCBT and PCBT were found to be 65.4, 71.8, 75.5% for optimum concentrations of 18, 16 and 12 ppm respectively. Other individual inhibitors such as Zn²⁺ and 3-PPA showed maximum inhibition efficiencies of 68.4 and 66.2%, respectively, for

the corresponding optimum concentrations of 75 and 12 ppm.

Various electrochemical parameters were calculated from Tafel plots and are given in Tables 3 and 4. It is clear that the i_{corr} values decrease significantly in the presence of derivatives other than BTA (Table 4). Further, the binary combination of each benzotriazole derivative with Zn²⁺ is a more effective inhibitor than BTA.

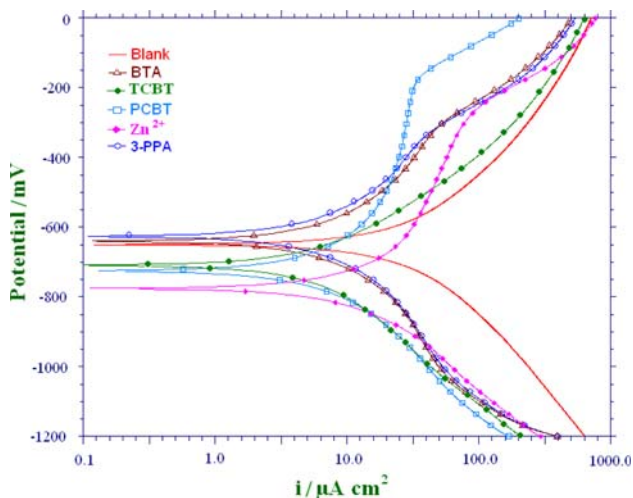


Fig. 2 Potentiodynamic polarization curves of mild steel in ground water in the presence and absence of optimum concentration of BTA, TCBT, PCBT, 3-PPA and Zn²⁺

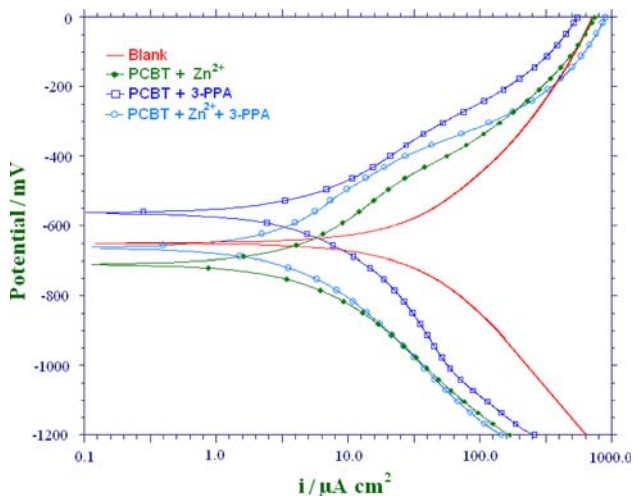


Fig. 3 Potentiodynamic polarization curves of mild steel in ground water in the presence and absence of optimum concentration of PCBT + 3-PPA, PCBT + Zn²⁺, and PCBT + Zn²⁺ + 3-PPA

The inhibition efficiencies were calculated from the polarization data using,

$$IE\% = \frac{i_{\text{corr}} - i'_{\text{corr}}}{i_{\text{corr}}} \times 100 \tag{2}$$

where, i'_{corr} and i_{corr} are the corrosion current densities with and without inhibitor, respectively.

Polarization results showing the influence of Zn²⁺ and 3-PPA with the benzotriazole derivatives on mild steel corrosion are presented in Table 4. In the presence of Zn²⁺ and 3-PPA, the efficiency of TCBT and PCBT is increased to 84.2 and 90.0% respectively. Correlating the values obtained for individual inhibitors with that of the combinations, it is evident that the addition of Zn²⁺ and 3-PPA to the benzotriazole derivatives controls the cathodic and anodic reactions. It can be concluded that benzotriazole derivatives act as mixed type inhibitors.

Initially benzotriazole compounds are adsorbed on the metal surface and after the addition of 3-PPA, Fe(II)-phosphonate complex is formed as a protective layer which enhances the corrosion inhibition efficiency. This confirms that the combination of benzotriazole compounds, Zn²⁺ and 3-PPA provides enhanced corrosion inhibition.

3.2.2 Electrochemical impedance studies

Typical Nyquist and Bode plots obtained for mild steel immersed at open circuit potential for 60 min at the optimum inhibitor concentration are shown in Fig. 3. The equivalent circuit used in this study is shown in Fig. 4. The resistance R_s represents ohmic resistance, R_1 represents the resistance to charge transfer due to oxidation of the metal and the phase constant element (CPE) corresponds to the double layer capacitance. The second subsystem R_2 corresponds to the resistance and C represents the capacitance of the inhibitor film on the metal surface due to adsorption. The values of the different elements present in the equivalent circuit were evaluated

Table 4 Potentiodynamic polarization parameters of mild steel in ground water containing optimum concentration of BTA + Zn²⁺, TCBT + Zn²⁺, PCBT + Zn²⁺, TCBT + Zn²⁺ + 3-PPA and PCBT + Zn²⁺ + 3-PPA

S. No.	Inhibitor	Inhibitor conc. (ppm)	E_{corr} (mV)	i_{corr} ($\mu\text{A cm}^{-2}$)	Corrosion rate (mpy)	Inhibition efficiency (%)
1	Blank	–	–640	12.59	6.0	–
2	BTA + Zn ²⁺	18 + 75	–696	3.30	1.6	73.8
3	TCBT + Zn ²⁺	16 + 75	–740	2.88	1.4	77.1
4	PCBT + Zn ²⁺	12 + 75	–735	2.51	1.2	80.0
5	PCBT + PPA	12 + 12	–555	2.44	1.1	80.1
6	TCBT + Zn ²⁺ + 3-PPA	16 + 75 + 12	–680	1.99	0.9	84.2
7	PCBT + Zn ²⁺ + 3-PPA	12 + 75 + 12	–655	1.26	0.6	90.0

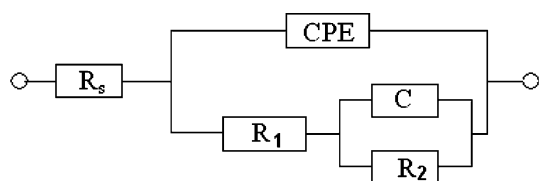


Fig. 4 Equivalent circuit

using a fitting procedure [21] and the parameters obtained are shown in Table 5 (Figs. 5, 6).

From the impedance plots of the individual inhibitors (BTA, TCBT, PCBT, Zn^{2+} and 3-PPA), it is evident that the values of charge transfer resistance increase in the order $BTA < TCBT < PCBT$, when compared to the blank, while the capacitance values decrease as $BTA > TCBT > PCBT$. This trend indicates that the inhibitors cover the surface of the metal due to adsorption thereby reducing the capacitive effects. For PCBT and Zn^{2+} combination further increase in the charge transfer resistance is noted and this value reaches a maximum for PCBT, Zn^{2+} and 3-PPA mixture ($1.7179 \times 10^4 \Omega$), demonstrating that this combination provides maximum corrosion protection. This fact is further substantiated from the decrease in double layer capacitance ($2.90 \mu F$) for PCBT, Zn^{2+} and 3-PPA mixture since lower values of double layer capacitance indicate thickening of the inhibitor film. All the ac measurements show the same trend as those observed from weight loss measurements and dc polarization.

3.3 Surface examination results

3.3.1 FT-IR spectra

A transmission vibrational spectrum of PCBT is depicted in Fig. 7. A broad peak at $3,317 \text{ cm}^{-1}$ indicates the

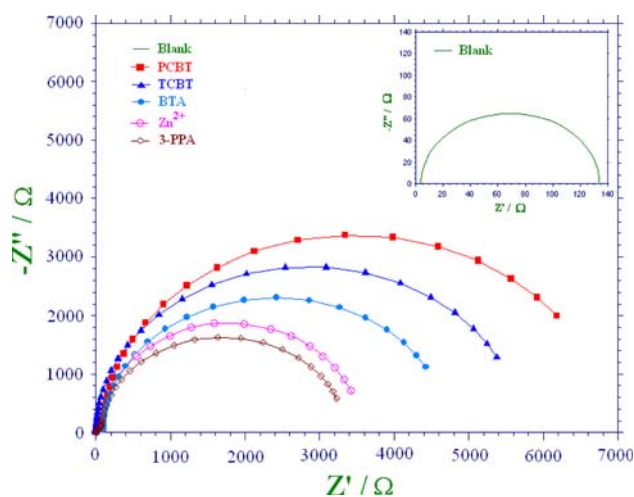


Fig. 5 Nyquist plot of mild steel in ground water in the presence and absence of optimum concentration of BTA, TCBT, PCBT, Zn^{2+} and 3-PPA

presence of the N–H bond of the pyrrole ring and the appearance of a peak in the region of $1,673 \text{ cm}^{-1}$ corresponds to the C=O symmetric stretching vibration of the carbonyl group. The presence of C–N stretching frequency is clearly manifest in the region $1,200$ to $1,020 \text{ cm}^{-1}$. Further peaks at $1,531$ to $1,450 \text{ cm}^{-1}$ can be attributed to the (N=N) group present in the ring and the C=C ring stretching peak appears at $1,415$ to $1,360 \text{ cm}^{-1}$. The peaks for C–N stretching modes can be assigned in the region around $1,150 \text{ cm}^{-1}$. The band at 800 – 600 cm^{-1} can be assigned to C–S stretching vibration of the thienyl group present in TCBT.

The reflectance FT-IR spectra obtained for the mild steel specimens immersed in groundwater containing the combination of inhibitors PCBT + Zn^{2+} and PCBT + Zn^{2+} + 3-PPA is presented in Fig. 8a, b. This shows the characteristic bands for the adsorbed benzotriazole derivatives on

Table 5 Electrochemical impedance parameters of mild steel in ground water with optimum concentration of various inhibitors

Inhibitors	C_{dl} (μF)	$R_{ct} \times 10^4$ (Ω)	Total impedance $\times 10^3$ (Ω)
Blank	15.03	0.0130	0.134
BTA	7.20	0.4120	4.420
TCBT	7.05	0.4549	5.370
PCBT	6.49	0.5728	6.214
Zn^{2+}	7.42	0.3981	3.815
3-PPA	7.33	0.3349	3.223
BTA + Zn^{2+}	6.19	0.9635	9.216
TCBT + Zn^{2+}	6.11	1.2589	10.58
PCBT + Zn^{2+}	5.81	1.2823	11.44
PCBT + 3-PPA	5.63	1.2916	11.78
TCBT + Zn^{2+} + 3-PPA	3.50	1.3820	13.22
PCBT + Zn^{2+} + 3-PPA	2.90	1.7179	15.89

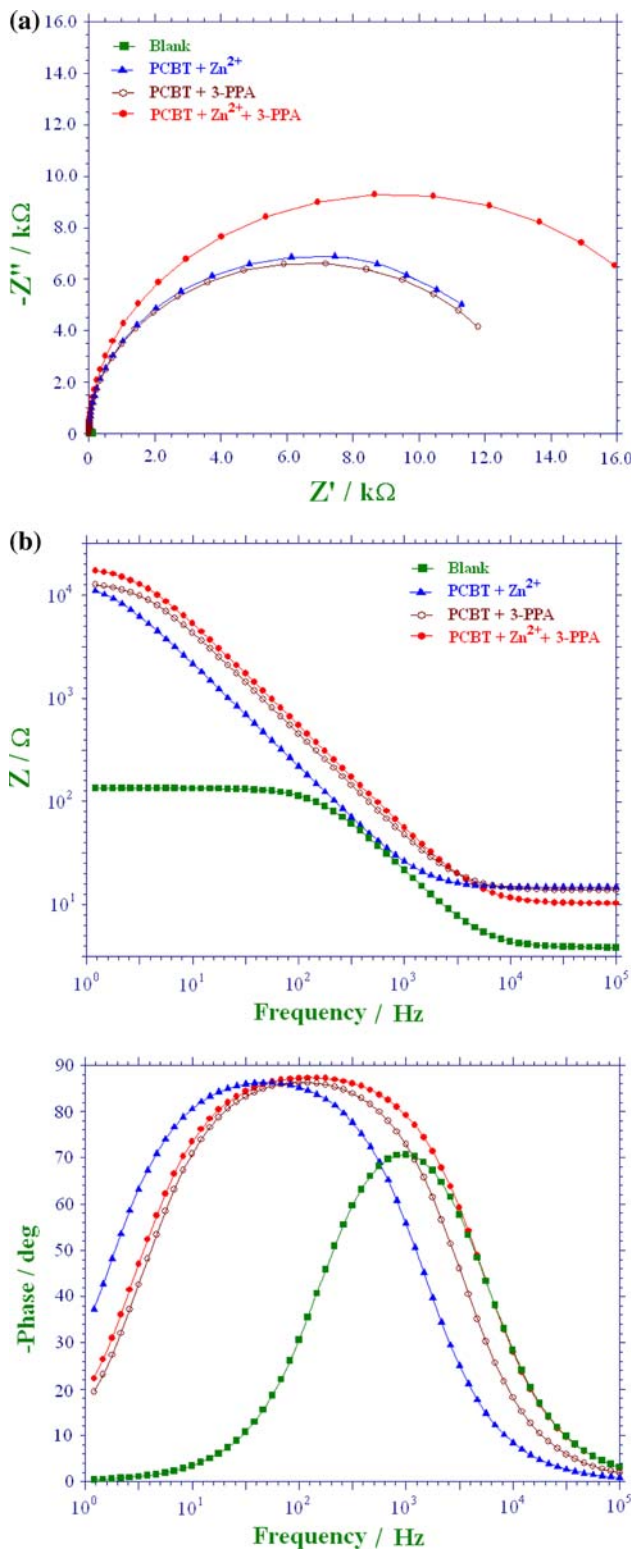


Fig. 6 **a** Nyquist plot of mild steel in ground water in the absence and presence of optimum concentration of PCBT + Zn²⁺, PCBT + 3-PPA and PCBT + Zn²⁺ + 3-PPA. **b** Bode plot of mild steel in ground water in the presence and absence of optimum concentration of PCBT + Zn²⁺, PCBT + 3-PPA and PCBT + Zn²⁺ + 3-PPA

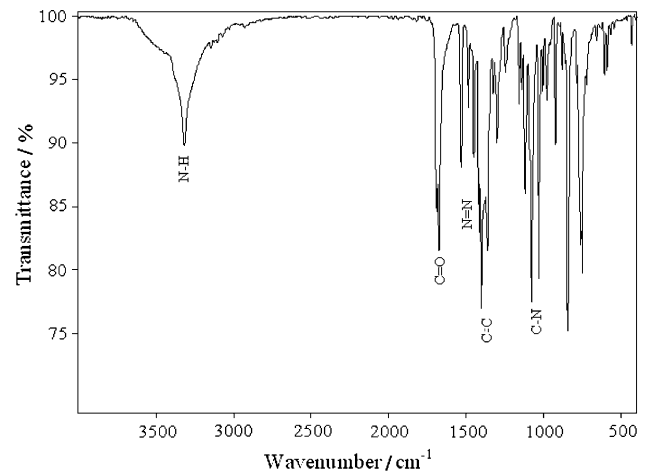


Fig. 7 FTIR transmittance spectrum of PCBT

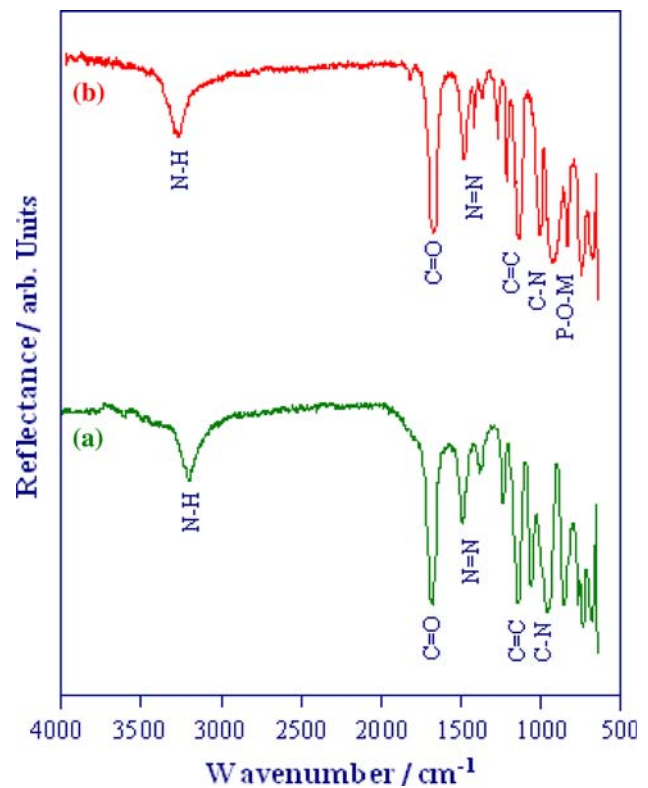


Fig. 8 Infrared reflectance spectra of mild steel immersed in ground water containing optimum concentration of **(a)** PCBT + Zn²⁺ and **(b)** PCBT + Zn²⁺ + 3-PPA

the metal surface. A broad band in the range 3,000–3,500 cm⁻¹, can be assigned to the presence of N–H. The presence of C=O, N=N, C=C and C–N is indicated by their stretching modes at 1690, 1500–1450, 1390 and 1120 cm⁻¹ respectively. For the system containing 3-PPA along with PCBT an additional band is observed that is

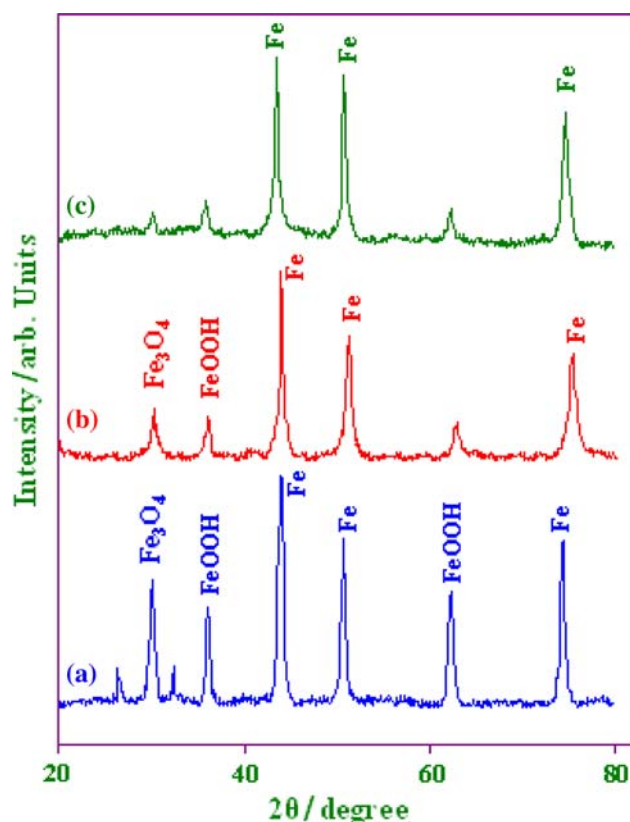


Fig. 9 XRD pattern obtained on the surface film formed on mild steel immersed in ground water environment (a) blank, (b) PCBT + Zn²⁺, (c) PCBT + Zn²⁺ + PPA

characteristic of an iron–phosphonate complex (i.e., the band at 985 cm⁻¹).

3.3.2 X-ray diffraction patterns

The XRD patterns of the corrosion products give qualitative information about the possible phases present. The patterns obtained clearly reveal the presence of metal and metal oxide phases. The XRD results are presented in Fig. 9 (a–c). The peak due to iron appears at $2\theta = 43.6^\circ$, 50.7° and 74.3° . Peaks at $2\theta = 30.2^\circ$, 35.8° and 62.2° can be assigned to oxides of iron. Thus, the surface of the metal immersed in ground water contains Fe₃O₄ and FeOOH. The XRD pattern for the metal immersed in the ground water containing optimum concentration of PCBT + Zn²⁺ + 3-PPA is given in Fig. 9c. The intensity of the peaks due to oxides of iron, such as Fe₃O₄ and FeOOH, are found to be very low and the peaks due to iron alone observed at $2\theta = 43.5^\circ$, 50.6° and 74.1° are very high.

4 Conclusions

1. The addition of PCBT and TCBT to corrosive ground water offer corrosion inhibition under specific experimental conditions.
2. The synthesized benzotriazole derivatives were found to suppress both anodic and cathodic reactions and hence behave as mixed type inhibitors.
3. Results obtained from weight loss measurements and electrochemical measurements are in good agreement.
4. The PCBT + Zn²⁺ + 3-PPA formulation shows the highest inhibition efficiency.
5. Surface analysis reveals the presence of an adsorbed film of benzotriazole derivative and Fe(II)–phosphonate complex on the mild steel immersed in PCBT + Zn²⁺ + 3-PPA system.

Acknowledgements The authors express sincere appreciation for financial support from the University Grants Commission (UGC), New Delhi, India (F. No. 32-206/2006 (SR)).

References

1. Tadros AB, Abdenaby BA (1988) J Electroanal Chem 246:433
2. Chin RJ, Nobe KJ (1971) J Electrochem Soc 118:545
3. Agrawal R, Nambodhiri TKG (1992) J Appl Electrochem 22:383
4. Eldakar N, Nobe K (1976) Corrosion 32:128
5. Mernari B, ElAttari H, Traisnel M, Bentiss F, Lagrenée M (1998) Corros Sci 40:391
6. Oneal C Jr, Borger RN (1976) Mater Perform 15:9
7. Xue G, Ding J (1990) Appl Surf Sci 40:327
8. Chadwick D, Hashemi T (1978) Corros Sci 18:39
9. Tornkvist C, Thiery D, Bergam J, Liedberg B, Leygraf C (1989) J Electrochem Soc 136:58
10. Xue G, Ding J, Lu P, Dong J (1991) J Phys Chem 95:7380
11. Walker R (1975) Corrosion 31:97
12. Gopi D, Manimozhi S, Govindaraju KM, Manisankar P, Rajeswari S (2007) J Appl Electrochem 37:439
13. Gopi D, Govindaraju KM, Manimozhi S, Ramesh S, Rajeswari S (2007) J Appl Electrochem 37:681
14. Ferreday D, Mitchell PJ, Wilcox GD, Greaves B (1993) Brit Corros J 28:185
15. Kalman E, Varhegyi B, Bako I, Felhosi I, Karman FH, Shabar A (1994) J Electrochem Soc 14:3357
16. Gopi D, Rajeswari S (2002) J Solid State Electrochem 6:194
17. Katritzky AR (2004) J Org Chem 69:6617
18. Wang X, Zhang Y (2003) Tetrahedron Lett 59:4201
19. Wang X, Zhang Y (2002) Tetrahedron Lett 43:5431
20. Langelier WF (1936) J Am Wat Works Assoc 28:1500
21. Basics of AC impedance measurements, Application note-AC-1, Egand G. Princeton Applied Research, Electrochemical Instrument Division, Princeton, NJ, 1982, 168